18th IFHTSE CONGRESS
International Federation for Heat Treatment and Surface Engineering
IFHTSE
ANAIS
PROCEEDINGS
ISSN 1516-392X

THE INFLUENCE OF PLASMA NITRIDING ON THE FATIGUE BEHAVIOR OF AUSTENITIC STAINLESS STEEL TYPES AISI 316 AND AISI 304[1]

Rogério Varavallo[2]
Marcos Dorigão Manfrinato[3]
Luciana Sgarbi Rossino[4]
Dirceu Spinelli[4]
Rosamel Melita Muñoz Riofano[4]
Sylvio Dionysio de Souza[5]

Abstract
The plasma nitriding process has been used as an efficient method to optimize the surface properties of steel and alloy in order to increase their wear, fatigue and corrosion resistance. This paper reports on a study of the composition and influence of the nitrided layer on the high-cycle fatigue properties of the AISI 316 and 304 type austenitic stainless steels. Test specimens of AISI 316 and 304 steel were nitrided at 400ºC for 6 hours under a pressure of 4.5 mbar, using a gas mixture of 80% volume of H_2 and 20% volume of N_2. The rotary fatigue limit of both nitrided and non-nitrided steels was determined, and the effect of the treatment on the fatigue limit of the two steels was evaluated. The mechanical properties of the materials were evaluated based on tensile tests, and the nitrided layer was characterized by microhardness tests, scanning electron microscopy and X-ray diffraction. The resulting nitride layer showed high hardness and mechanical strength, increasing the fatigue limit of the nitrided material in comparison with the non-nitrided one. The fatigue limit of the 316 steel increased from 400 MPa to 510 MPa in response to nitriding, while that of the 304 steel increased from 380 MPa to 560 MPa. One of the contributing factors of this increase was the introduction of residual compressive stresses during the surface hardening process, which reduce the onset of crack formation underneath the nitride layer.
Keywords: Plasma nitriding; Type 316 and 304 austenitic stainless steel; Fatigue.

INFLUÊNCIA DA NITRETAÇÃO A PLASMA NO COMPORTAMENTO EM FADIGA DOS AÇOS INOXIDÁVEIS AUSTENÍTICOS AISI 316 E AISI 304

Resumo
O processo de nitretação a plasma tem sido utilizado como um método eficiente para otimizar as propriedades superficiais de aços e ligas metálicas com o objetivo de elevar a resistência ao desgaste, à fadiga e à corrosão. Neste trabalho, estudou-se a composição e a influência da camada nitretada nas propriedades de fadiga de alto ciclo dos aços inoxidáveis austeníticos AISI 316 e 304. Corpos de prova de aço AISI 316 e 304 foram nitretados a 400°C durante 6 horas, com pressão de 4,5 mbar, utilizando uma mistura gasosa de 80% em volume de H_2 e 20% em volume de N_2. Determinou-se o limite de fadiga rotativa para os dois materiais estudados, nitretados e não nitretados, observando-se o efeito do tratamento no limite de fadiga de ambos os materiais. As propriedades mecânicas dos materiais foram determinadas através de ensaios de tração, e a camada nitretada foi caracterizada através de ensaios de microdureza, microscopia eletrônica de varredura e difração de raio-x. A camada de nitreto formada possui alta dureza e resistência mecânica, o que proporcionou aumento no limite de fadiga do material nitretado em relação ao não nitretado. O limite de fadiga do aço 316 aumentou de 400 MPa para 510 MPa após o tratamento de nitretação, enquanto que para o aço 304, o limite de fadiga aumentou de 380 MPa para 560 MPa. Um dos fatores que contribuiu para isto foi a introdução de tensões residuais compressivas durante o processo de endurecimento superficial, que retarda a iniciação da trinca. A análise fractográfica evidenciou a iniciação da trinca abaixo da camada de nitreto formada.
Palavras-chave: Nitretação a plasma; Aços austeniticos 316 e 304; Fatiga.

[1] *Technical contribution to the 18th IFHTSE Congress - International Federation for Heat Treatment and Surface Engineering, 2010 July 26-30th, Rio de Janeiro, RJ, Brazil.*
[2] *Master's student in Materials Science and Engineering, EESC, University of São Paulo, Brazil.*
[3] *M.Sc. in Materials Science and Engineering, EESC, University of São Paulo, Brazil.*
[4] *Ph.D. in Materials Science and Engineering, EESC, University of São Paulo, Brazil.*
[5] *Ph.D. in Materials Science and Engineering, UFSCAR, Federal University of São Carlos, Brazil.*

1 INTRODUCTION

The expression “stainless steel”, as it is commonly known, imparts the idea of a material that is indestructible even when subjected to the most varied corrosive environments. In truth, however, this material is not eternal, but usually displays high corrosion resistance when subjected to a given medium or aggressive agent. It is also more oxidation-resistant at high temperatures than other classes of steel.

The oxidation and corrosion resistance of stainless steel is due mainly to the presence of chromium, which, starting from a given amount and in contact with oxygen, allows for the formation of a film of chromium oxide on the steel’s surface, which is impermeable and insoluble in common corrosive media. Thus, stainless steel can be defined as a group of oxidation and corrosion-resistant low-carbon ferrous alloys that contain at least 12% of chromium.

In recent years, the study of the tribological properties of surfaces has become fundamental in innumerable industrial applications. There are several surface treatment techniques for improving the surface properties of materials, including mechanical, thermal, physical and chemical processes.

Plasma nitriding is one of the processes that use plasma-aided deposition, also known as ion nitriding.[1] This thermochemical process improves the material’s catalytic performance, resistance to corrosion, oxidation and adhesion, and surface mechanical properties such as hardness, fatigue, friction and wear resistance.[2-6]

The study of fatigue has gained increasing importance as technological advances spread to growing numbers of products such as automobiles, airplanes, compressors, pumps, turbines, etc., all of which are subjected to repeated loading and vibration.[7] According to the ASTM E 1150 standard, fatigue is defined as “a process of permanent structural, localized and progressive change that occurs in a material subjected to conditions that produce fluctuating stresses and deformations at some point (or points), which may culminate in cracks or complete fracture after a sufficient number of fluctuations.”

To increase the fatigue limit of any material requires the introduction of residual stresses on its surface. These residual stresses can be introduced through processes such as blasting with abrasive grains, surface rolling, cold deformation in fastener holes, heat treatment, and thermochemical treatment (plasma nitriding).[3,8,9] The layer of nitrides formed during the treatment has a positive influence on the fatigue life of a component for two main reasons.[9] The first is the delay in fatigue crack nucleation due to the increase in surface mechanical strength. The second reason has to do with the introduction of residual compressive stresses during the process of surface hardening, which retards the onset of cracks, reducing the stress intensity factor.[3,9,10]

Thus, the objective of this work was to study the composition of the nitride layer and the influence of this layer on the high-cycle fatigue properties of AISI 304 and 316 austenitic stainless steels with similar composition and microstructure.

2 MATERIALS AND METHODS

The materials under study were AISI 304 and AISI 316 austenitic stainless steels, which were received in the form of 2 m long, 12.75 m diameter bars. Their nominal

chemical compositions are listed in Table 1. The chemical analyses were carried out by the wet-chemical route.

Table 1. Nominal chemical composition of the AISI 304 and AISI 316 austenitic stainless steels (% in weight)

Steel	C	Si	Mn	P	S	Cr	Mo	Ni
304	0.08 max	1.0 max	2.0 max	0.045 max	0.08 max	18.0-20.0	-	8.0-10.5
316	0.08 max	1.0 max	2.0 max	0.045 max	0.03 max	16.0-18.0	2.0-3.0	10.0-13.5

The plasma nitriding treatments were carried out in a device composed of a chamber, a vacuum system, a gas distribution unit, a power source, and electronic pressure control valves. The schematic diagram in Figure 1 shows the main components of the system.

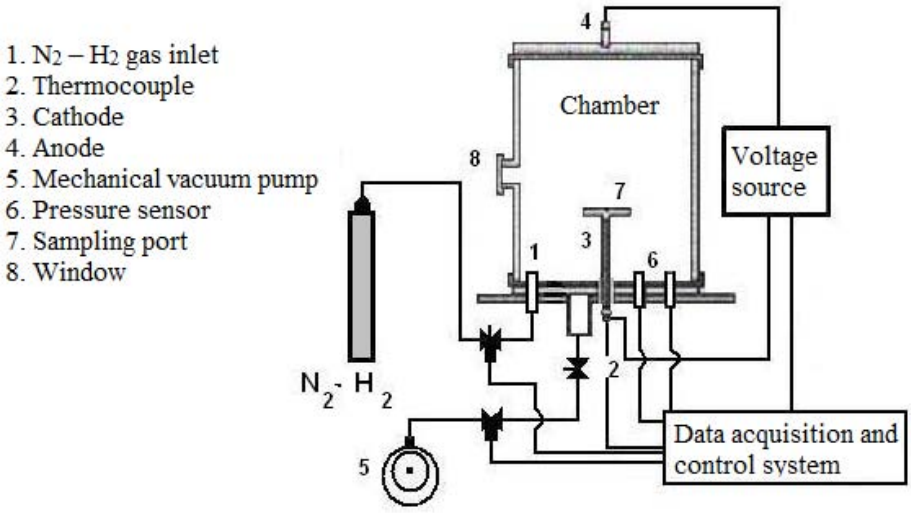

Figure 1. Schematic diagram of the plasma nitriding system.

The plasma nitriding system has a maximum output voltage of 850V, with a power of 5KVA, and can operate with direct or alternating current. When using alternating current, the frequency can be varied from 1 to 150 kHz and the work cycle from 10 to 100%. The process variables (time, temperature, pressure, and gas mixture) are monitored by a data acquisition and control system. In this work, 3 parameters were kept constant: temperature at 400°C, pressure of 4.5 mbar, and gas mixture of 80%H_2 and 20%N_2. The samples were nitrided for different times of 1, 3, 6 and 10 hours to determine the best treatment time.

The samples' microstructures were examined by scanning electron microscopy (SEM, Zeiss/Leica model 440). To this end, the samples were prepared as established by the E 395 standard,[11] embedded in phenolic resin, sandpapered with #220 to #1000 emery paper, and then polished with chromium oxide (10μm) and alumina oxide (2μm and 0.5μm). The nitrided layer was revealed with aqua regia etchant.

Vickers microhardness (HV) tests were performed on the surface region of the tested samples, using a Micromet series 2100 microhardness tester under a load of

25 gf. The tests were performed according to the ASTM 384-99 standard.[12] Hardness was measured before and after each plasma nitriding treatment. The surface hardness reported for each sample represents the mean of five impressions distributed over the entire sample.

X-ray diffraction analyses were carried out to identify the phases of the nitrided layer, using a Siemens D5000 diffractometer equipped with a graphite monochromator and CuK_{α} radiation tube. The measurements were taken in steps of 0.05º/2min, with 2θ varying from 30º to 120º.

Rotary bending fatigue tests were carried out as established by the ASTM E466-96 standard,[13] using a Fatigue Dynamics RFB-200 rotary bending machine. Non-nitrided and nitrided test specimens were tested. Five stress levels were applied in each testing condition, and 3 tests were performed for each stress level. A frequency used was 24.5Hz at room temperature. The tests were carried out up to failure of the test specimen, and test specimens reaching a life of 10^7 cycles (runout) were considered to have an infinite life. After the tests, the fractured surfaces were subjected to a fractographic analysis by SEM. The sketch in Figure 2 illustrates the dimensions of the rotary fatigue test specimen.

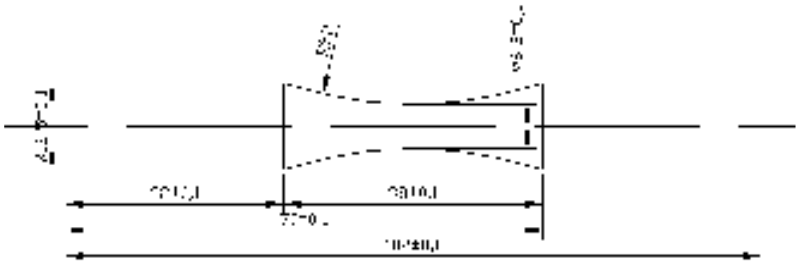

Figure 2. Geometry and dimensions of the rotary fatigue test specimen according to the ASTM E 466-96 standard.

3 RESULTS AND DISCUSSION

3.1. Chemical Analysis

The results of the compositions of the two steels listed in Table 2 meet the specifications of the ASTM A 276-02 standard. However, the chemical composition of the AISI 304 austenitic stainless steel should not contain molybdenum, as specified by the ASTM A 276-02 standard. This percentage of molybdenum undoubtedly originates from impurities in the scrap metal used in the alloy casting process.

Table 2. Chemical compositions (% in weight) analyzed by the wet route

Steel	C	Si	Mn	P	S	Cr	Mo	Ni
304	0.032	0.41	1.21	0.021	0.014	18.34	0.18	8.26
316	0.034	0.61	1.54	0.013	0.012	17.42	2.23	10.41

3.2 Analysis of the Nitrided Layer

Figures 3 and 4 depict the profile of the nitrided layer of the AISI 304 and AISI 316 steels, respectively. In the case of the AISI 304 austenitic stainless steel, nitriding times

of 6 hours and 10 hours resulted in a higher attack on the nitrided layer. In the case of the AISI 316 austenitic stainless steel, only the 10-hour treatment time produced corrosion points in the layer. The nitrided layer was found to consist of two distinct regions, an outer layer, called composite layer, composed of expanded austenite – S-phase, and a diffusion layer corresponding to the intermediate phase between the nitrided layer and the matrix. The thickness of the S-phase in both steels increased with increasing nitriding times, which is favorable because it makes the surface of the material harder and more wear resistant.

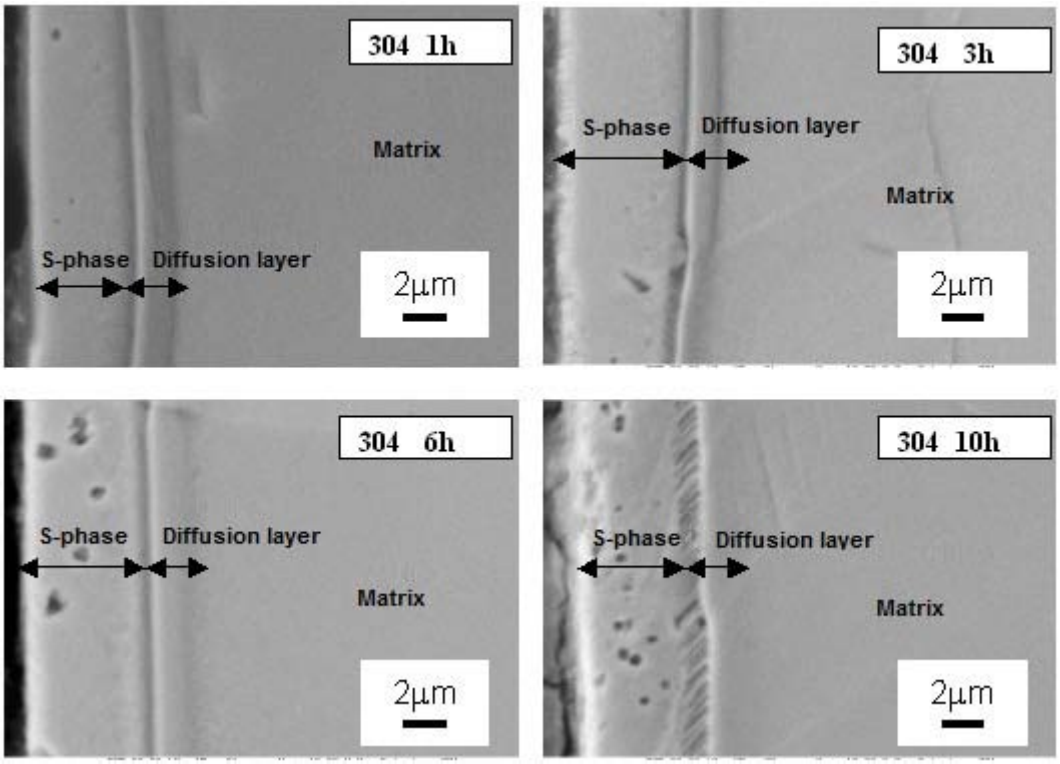

Figure 3. SEM micrographs of the AISI 304 austenitic stainless steel nitrided at 400ºC for 1, 3, 6 and 10 hours.

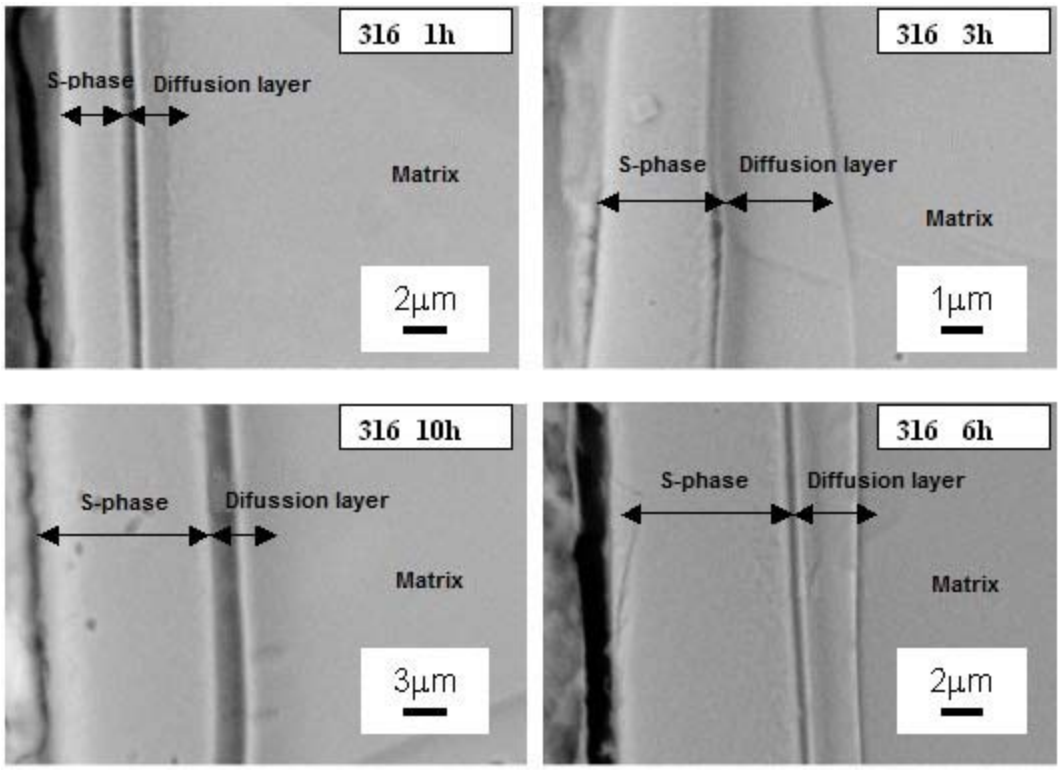

Figure 4. SEM micrographs of the AISI 316 austenitic stainless steel nitrided at 400ºC for 1, 3, 6 and 10 hours.

The depth of the nitrided layer as a function of treatment time was measured based on the SEM micrographs. Figure 5 depicts the results, showing that the growth of the total nitrided layer (composite + diffusion layers) on the steels is governed by mechanisms of diffusion, i.e., the depth of the nitrided layer increases proportionally to the nitriding time.

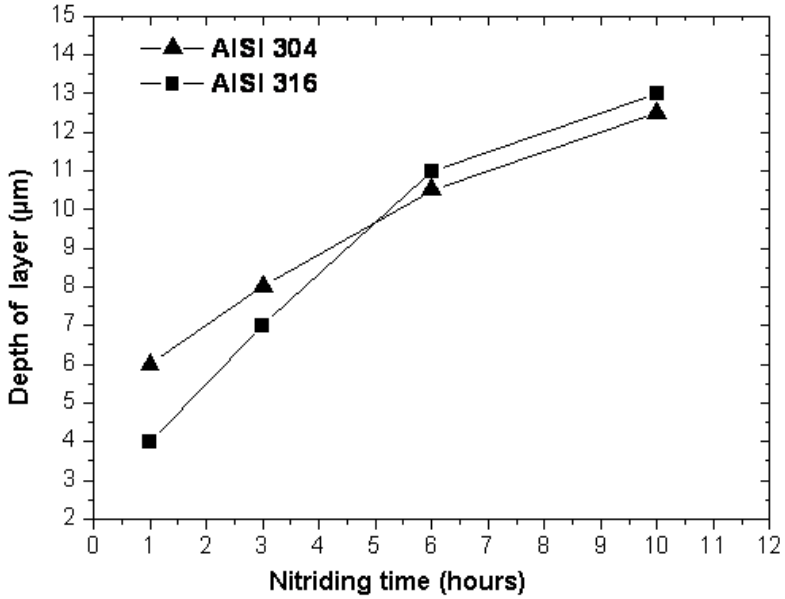

Figure 5. Depth of the nitrided layer (composite layer + diffusion layer) as a function of treatment time at a temperature of 400ºC.

The samples' microsurface hardness increased with nitriding time when compared to the hardness of the matrix, as indicated in Figure 6. This increase in hardness was due to the increment in the thickness of the S-phase. It was also found that treatment times of 6 and 10 hours resulted in very similar values of microsurface hardness.

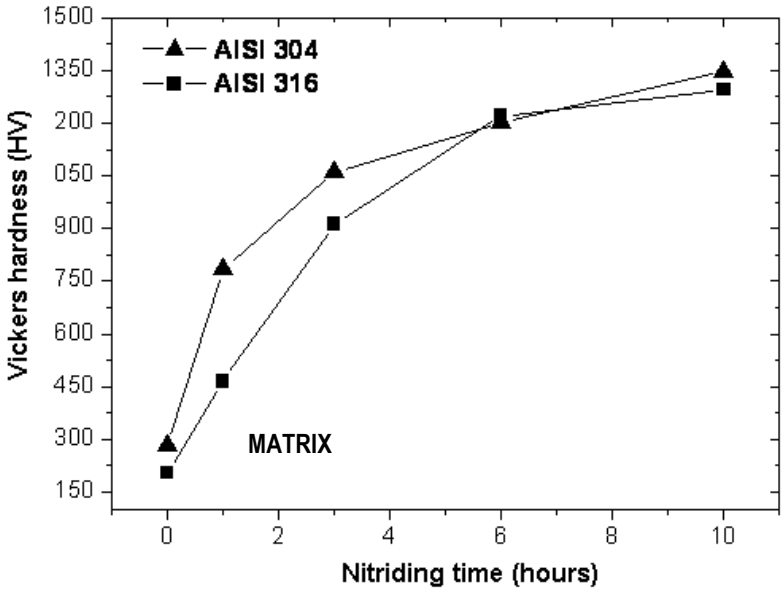

Figure 6. Microsurface hardness of nitrided layer as a function of nitriding time of AISI 304 and 316 austenitic stainless steels, using a load of 25 gf.

Figure 7 illustrates the X-ray diffraction results of samples nitrided at 400ºC for 1, 3, 6 and 10 hours. Note the variation in the intensities of the peaks corresponding to the nitrides formed during the. As can be seen, the surface layer is composed essentially of γ´-Fe_4N precipitates or S-phase, and shows two preferential orientations, the larger one being <111>, and the second, smaller one <200>. The results also show that nitrides were formed over the entire surface, since no intensity peak corresponding to the iron matrix was found, even after only 1 hour of nitriding.

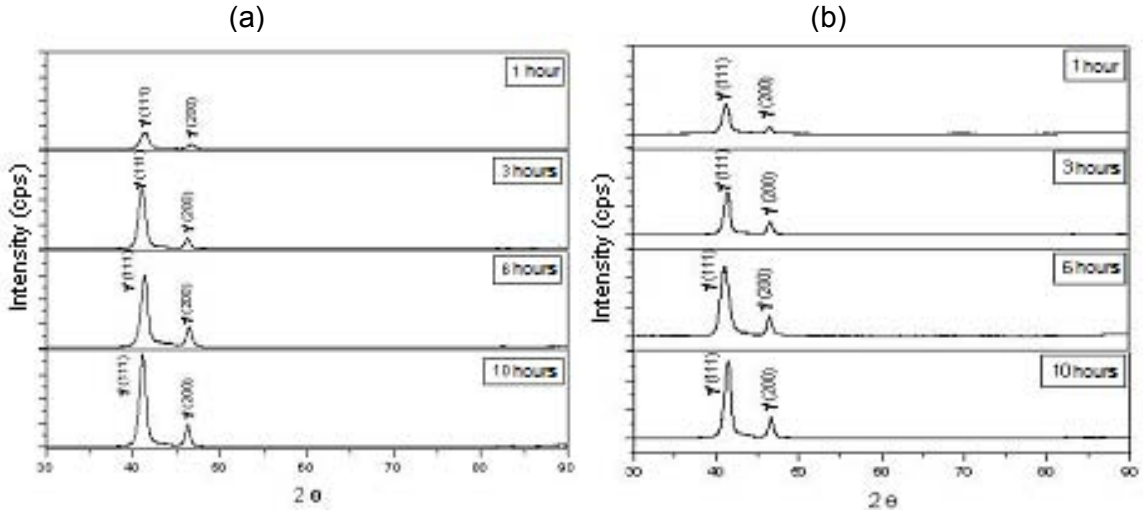

Figure 7. Diffractograms of austenitic stainless steel samples nitrided at 400ºC for 1, 3, 6 and 10 hours: (a) AISI 304 steel, (b) AISI 316 steel.

3.3 Rotary Bending Fatigue

Figure 8 shows the results of the rotary bending tests of the non-nitrided and nitrided test specimens of the two steels. The fatigue limits of the test specimens of non-nitrided and nitrided AISI 304 steel showed values of 380 MPa and 560 MPa, respectively, while those of the AISI 316 steel were 400MPa and 510MPa, respectively.

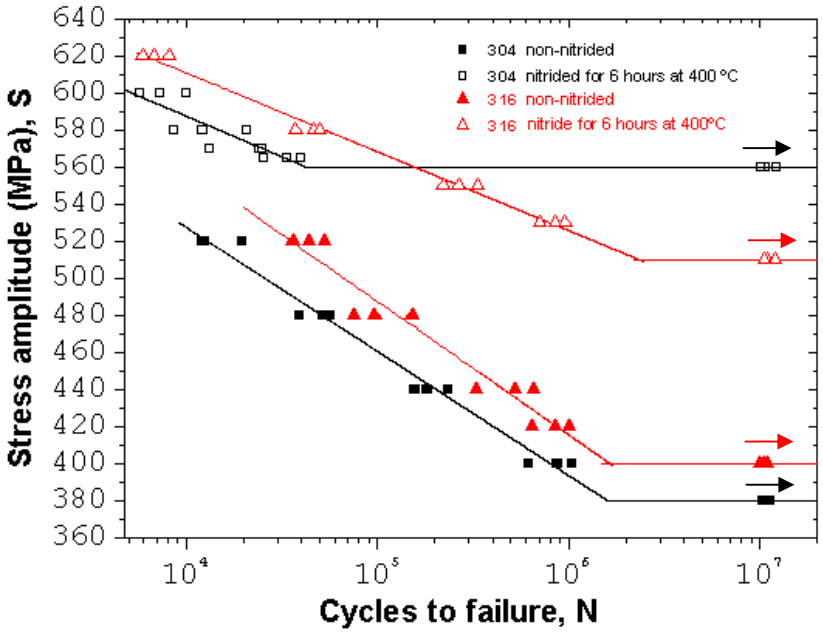

Figure 8. Comparison of the stress amplitudes as a function of the number of cycles to failure of the test specimens of non-nitrided and nitrided AISI 304 and 316 steels.

The stress amplitudes as a function of the number of cycles to failure shown in Figure 8 enabled us to determine and visualize the fatigue limits of the AISI 304 and 316 steels for each type of nitrided and non-nitrided test specimen. The non-nitrided test specimens of both steels showed very similar fatigue limit values, i.e., 380MPa for the AISI 304 steel and 400MPa for the AISI 316 steel. However, the nitrided test specimens showed a difference in their fatigue limits, with the AISI 304 steel presenting the higher value, 560 MPa, and the AISI 316 steel the lower one, 510 MPa.

A comparison of the results depicted in Figure 8 indicates that the fatigue limits of the nitrided test specimens increased in relation to the non-nitrided samples. This change in performance resulted from the introduction of residual compressive stresses that counteract the tensile stresses, making nucleation of surface cracks more difficult. Up to its fatigue limit of 560 MPa, the AISI 304 steel maintained the integrity of its nitrided layer. However, this integrity was impaired upon increasing the applied stress, leading to rapid fracture of the specimens. The AISI 316 steel showed the same behavior, i.e., the integrity of its nitrided layer was impaired above its fatigue limit of 510 MPa, albeit with a difference in that the test specimens fractured slowly under increasing stress, indicating that the integrity of the nitrided layer gradually loses its effectiveness.

Figures 9 to 13A show fractographic images of the fracture surfaces of the samples of non-nitrided AISI 304 steel (304-6A) stress-tested at 400 MPa and 617,400 cycles,

steel (304-9N) stress-tested at 600 MPa and 10,100 cycles, and samples of the AISI 316 steel (316-14N) stress-tested at 530 MPa and 708,400 cycles, and (316-9N) stress-tested at 620 MPa and 6,800 cycles.

Figure 9 illustrates the regions of crack nucleation (NU), stable propagation (SP) and unstable propagation or ultimate failure (UF). Only one region of crack nucleation is visible. An analysis of the fracture surface of the test specimen in Figure 9(a) reveals only one well defined region where the main site of crack propagation occurred.

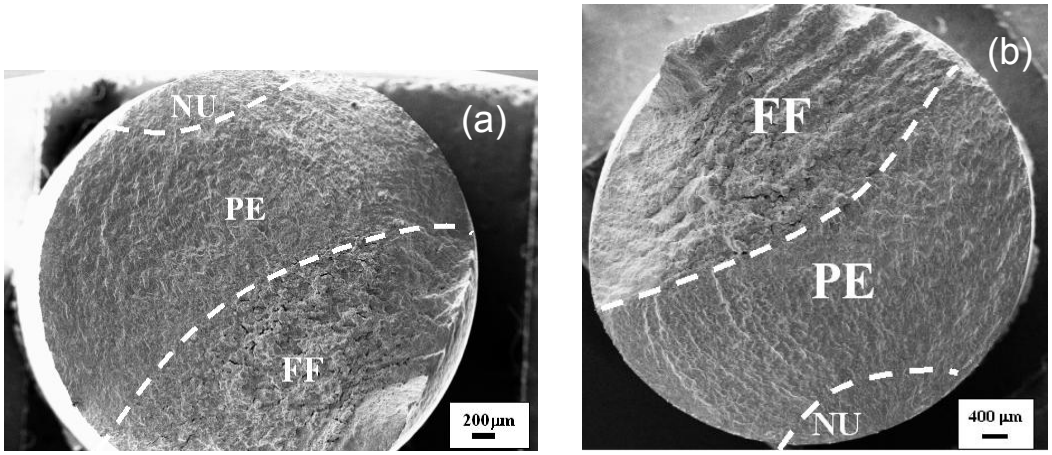

Figure 9. Macrographic aspect of the fracture surface of the test specimens, highlighting regions of crack nucleation (NU), stable propagation (SP) and ultimate failure (UF): (a) non-nitrided AISI 304 steel stress-tested under 400 MPa and fractured after 617,400 cycles; (b) nitrided AISI 316 steel stress-tested under 530 MPa and fractured after 708,400 cycles.

Thus, it was found that there are two forms of crack nucleation, one presenting a single nucleation site and the other with various nucleation sites. The non-nitrided steels, and the nitrided AISI 316 steel stress-tested below 530 MPa showed only one nucleation site. In contrast, the nitrided AISI 304 and AISI 316 steels stress-tested above 560 MPa showed several nucleated surface cracks starting from several nucleation sites, leading to a typical fracture surface called a ratchet surface, as illustrated in Figures 10(a) and 11(a). Cracking of the lateral surface, as can be seen in Figures 10(b) and 11(b), resulted from the high stress applied to the specimen, i.e., from the high bending moment acting upon the lateral surface, which caused the nitrided layer to break to accommodate the deformation to which the test specimen was subjected. Note, also, that at stresses below 560 MPa, neither of the nitrided steels showed this ratchet marking behavior, since this level of stress is insufficient to cause cracking of the nitrided layer. Therefore, in this case, the compressive stresses originated by the nitrided layer the peak of tensile stress during the test to shift to a sub-surface region, which is responsible for the single crack nucleation site, as depicted in Figures 12(a) and (b).

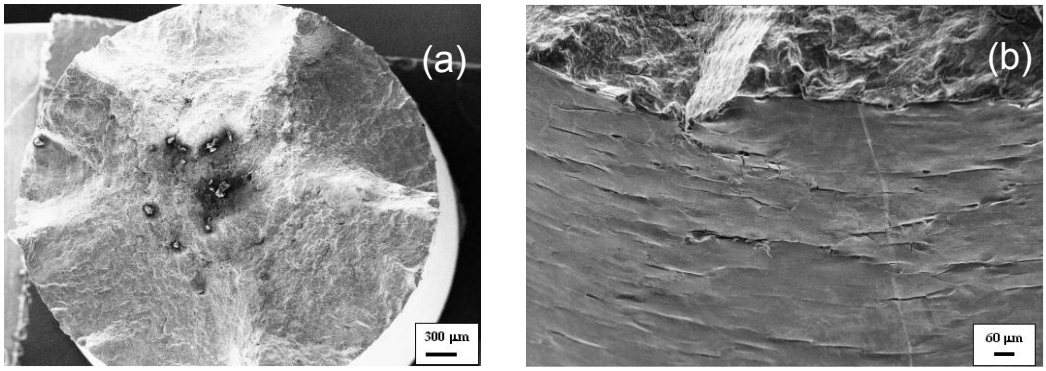

Figure 10. Macrographic aspect of the fracture surface of the nitrided AISI 304 steel test specimen stress-tested at 600 MPa and fractured after 10,100 cycles: (a) fracture surface showing ratchet marks; (b) lateral surface of a nucleation site. The presence of numerous microcracks on the surface of the nitrided layer gives rise to various nucleation sites in the fracture region.

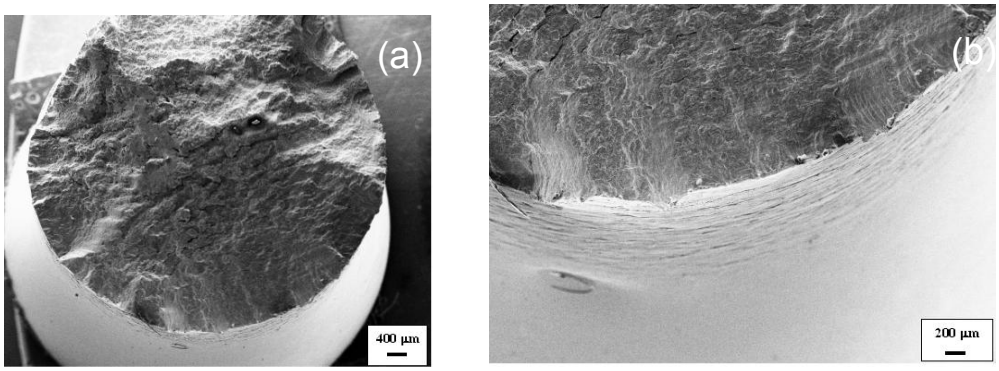

Figure 11. Macrographic aspect of the fracture surface of the nitrided AISI 316 steel test specimen stress-tested at 6200 MPa and fractured after 6,800 cycles: (a) fracture surface showing ratchet marks, demonstrating the nucleation of multiple cracks occurred in the material, which, upon joining, formed steps in the fracture surface; (b) overview of the lateral surface and a group of nucleation sites, with presence of microcracks on the surface of the nitrided layer.

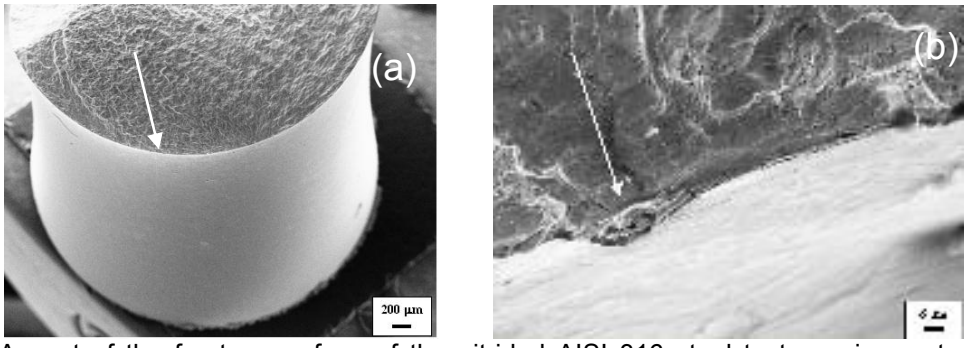

Figure 12. Aspect of the fracture surface of the nitrided AISI 316 steel test specimen stress-tested at 530 MPa and fractured after 708,400 cycles: (a) overview of the lateral surface without microcracks, and of the nucleation site, indicated by the arrow; (b) general view of the nucleation site close to the nitrided layer, indicated by the arrow.

Figure 13 clearly shows the presence of stage II fatigue crack propagation striae, spaced at intervals of 0.5 µm. Inclusions were also found, as indicated by an arrow. Figure 13 shows the same stage II fatigue striae, albeit receding. This phenomenon is caused by mechanical contact between the fractured parts of the test specimen when they are in the compression cycle during the test, prior to ultimate fracture.

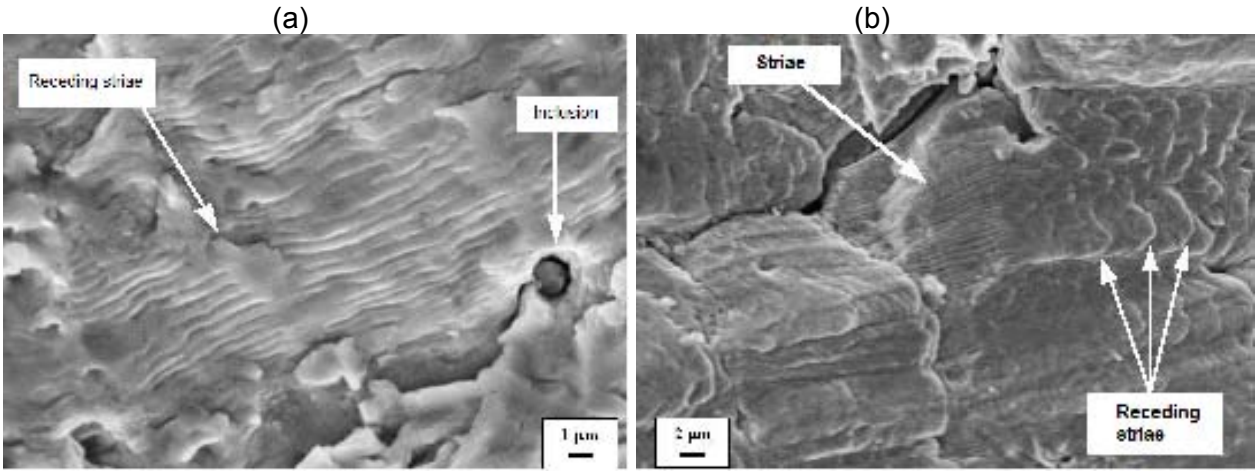

Figure 13. Macrographic aspect of the fracture surface of the test specimens: (a) non-nitrided AISI 304 stress-tested at 400 MPa in 617,400 cycles. Detailed view of the stage II crack propagation striae, spaced at intervals of 0.5 μm; (b) nitrided AISI 316 stress-tested at 530 MPa and fractured in 708,400 cycles. Striae, and striae receding due to mechanical contact of the test specimen under compression. Image recorded in the region close to the site of ultimate fracture.

4 CONCLUSIONS

- The plasma nitriding process offers an alternative for improving the properties of AISI 304 and 316 austenitic stainless steels.
- The depth and microsurface hardness of the nitrided layer increased along with increasing nitriding time, reaching a mean depth of 11 μm and a mean hardness of 1200 HV after 6 hours of treatment.
- The layer of nitrides formed on both steels nitrided at 400ºC for 6 hours presented only γ'-Fe_4N phase, and the X-ray diffraction peaks that characterize this phase and that occur in the family of planes <111> and <200> differ only in intensity, showing higher intensity in the AISI 316 steel in both families of planes.
- The fatigue limits of the nitrided AISI 304 and 316 steels increased by 47% and 27.5%, respectively, when compared with those of the steels in the as-received condition. This is due to the introduction of residual compressive stresses caused by the existence of the nitrided layer, which indirectly retards the fatigue crack nucleation process, thus increasing the steels' fatigue resistance.

REFERENCES

1 G. F. Gomes, M. Ueda, H. Reutauer. Alternated high and low pressure nitriding of austenitic stainless steel: Mechanisms and results. Journal of Applied Physics. Volume 94, nº 8, páginas 5379-5383, October 2003.

2 K. Genel, M. Demirkol, M. Capa. Effect of íon nitriding on fatigue behaviour os AISI 4140 steel. Materials Science and Engineering A, Volume 279, páginas 207-216, ano 2000.

3 N. Limodin, Y. Verreman, N. Tarfa. Axial fatigue of a gas nitrided quenched and tempered AISI 4140 steel: effect of nitriding depth. Fatigue Fracture Engineering Materials Structure. Volume 26, páginas 811-820, ano 2003.

4 N. Limodin, Y. Verreman, N. Tarfa. Axial fatigue of a gas nitrided quenched and tempered AISI 4140 steel: effect of nitriding depth. Fatigue Fracture Engineering Materials Structure. Volume 26, páginas 811-820, ano 2003.
5 R. Grün, H. J. Günther. Plasma nitriding in industry – problems, new solutions and limits. Materials Science and Engineering A, Volume 140, páginas 435-441, ano 1991.
6 Daniewcz, S.R.; Morre, D.H. Increasing the beding fatigue resistance of spur gear teeth using a presetting process. International Journal of Fatigue, v20, n7, p537-542, 1998.
7 G. E. Dieter. Metalurgia mecânica. Segunda edição Rio de Janeiro 1981.
8 V. Chiaverini. Tecnologia mecânica – Estrutura e propriedades das ligas metálicas. Volume 2, 2º edição. 1986. Makron books do Brasil Editora Ltda.
9 B. W. Hwang, C. M. Suh, H. K. Jang. Effects of surface hardening and residual stress on the fatigue characteristics of nitrided sacm 645 steel. International Journal of Modern Physics B. volume 17, páginas 1633-1639, ano 2003.
10 A. Alsaran, M. Karakan, A. Çelik. The investigation of mechanical properties of íon nitrided AISI 5140 low alloy steel. Materials Characterization, Volume 48, páginas 323-327, ano 2002.
11 American Society for Testing and Materials – ASTM E 3–95. Standard practice for preparation of metallographic specimens. West Conshohocken, ASTM, 2000.
12 American Society for Testing and Materials – ASTM E 384-99. Standard test method for microindentation hardness of materials. West Conshohocken, ASTM, 2000.
13 American Society for Testing and Materials – ASTM E 466–96. Standard practice for conducting force controlled constant amplitude axial fatigue tests of metallic materials. West Conshohocken, ASTM, 2000.